

Evaluation of electronic state of $\text{Mg}_4(\text{Nb}_{2-x}\text{Sb}_x)\text{O}_9$ microwave dielectric ceramics by first principle calculation method

Hirotaoka Ogawa^a, Hidekazu Taketani^a, Akinori Kan^{a,*}, Akihiro Fujita^b, Georgios Zouganelis^c

^a Department of Transportation Engineering, Meijo University, 1-501 Shiogamaguchi, Tempaku-ku, Nagoya 468-8502, Japan

^b Department of Civil Engineering, Meijo University, 1-501 Shiogamaguchi, Tempaku-ku, Nagoya 468-8502, Japan

^c Japan Fine Ceramics Center, 2-4-1 Mutsuno, Atsuta-ku, Nagoya 456-8587, Japan

Abstract

The microwave dielectric properties of $\text{Mg}_4(\text{Nb}_{2-x}\text{Sb}_x)\text{O}_9$ (MNS) solid solutions were evaluated and the variations in the electric state of the solid solutions were also investigated by using the first principle calculation method. The formation of a single phase was observed from the X-ray powder diffraction patterns of the solid solutions sintered at 1400 °C in the composition x from 0 to 1. The MgO and $\text{Mg}_7\text{Sb}_2\text{O}_{12}$ compounds were detected as the secondary phases at the compositions higher than $x = 1$; therefore, this result is closely related to the vaporization of Sb in this composition range. When comparing the overlap population of the $(\text{NbMg}_{12}\text{O}_{45})^{-61}$ cluster model with that of the $(\text{SbMg}_{12}\text{O}_{45})^{-61}$ cluster model, the slight covalency of the Sb–O bond was recognized from the results of the first principle calculation method. In the composition range of 0–1, the $Q \cdot f$ values of MNS sintered at 1400 °C increased from 196,000 to 280,000 GHz; the dielectric constants of the solid solutions ranged from 13 to 10. However, an improvement in the temperature coefficient of resonant frequency with the Sb substitution for Nb was not recognized.

© 2005 Elsevier Ltd. All rights reserved.

Keywords: Powders-solid state reaction; X-ray method; Dielectric properties; Niobates

1. Introduction

For a wireless communication system at a high frequency, the microwave dielectric ceramics are required to have a high quality factor ($Q \cdot f$), a near zero temperature coefficient of resonant frequency (τ_f) and a dielectric constant (ϵ_r) which is suitable for the application. In addition to the microwave dielectric properties as mentioned above, it is also necessary to consider a cost. The commercially utilized high- Q material such as Al_2O_3 have a high sintering temperature.¹ Thus, there is considerable interest in the development of new microwave dielectric ceramics with high $Q \cdot f$ value that can be used for the high frequency microwave devices. Recently, Ogawa et al.² reported the microwave dielectric properties of a corundum-type of $\text{Mg}_4(\text{Nb}_{2-x}\text{Ta}_x)\text{O}_9$ (MNT) solid solutions; it was found that the $Q \cdot f$ values of the solid solutions increased with the substitution of Ta for

Nb ($(Q \cdot f)_{\text{max}} = 347,000$ GHz at $x = 2$). Moreover, from the results of crystal structure analysis and first principle calculation of the solid solutions, it was suggested that the Ta substitution for Nb exerted an influence on the increase in the covalency of the Ta–O bond, though the remarkable variations in the covalency of Mg–O bond were not observed with the Ta substitution for Nb. In the case of the V substitution for Nb in a $\text{Mg}_4\text{Nb}_2\text{O}_9$ (MN) compound, a small amount of V ($x < 0.125$) was substituted for Nb, and the sintering temperature of $\text{Mg}_4(\text{Nb}_{2-x}\text{V}_x)\text{O}_9$ (MNV) solid solutions was extremely reduced from 1350 to 1025 °C, showing the maximum $Q \cdot f$ value of 165,000 GHz at the sintering temperature of 1050 °C.³

As for the possibility of another element substituting for Nb in MN, the element of Sb is considered to be an appropriate candidate for the substitution because the ionic radius of Sb^{5+} ion (0.6 Å) is similar to that of the Nb^{5+} (0.65 Å) ion.⁴ Thus, the $\text{Mg}_4(\text{Nb}_{2-x}\text{Sb}_x)\text{O}_9$ (MNS) solid solutions were prepared; the influences of the Sb substitution for Nb on the electrical and crystal structures, and the microwave

* Corresponding author.

E-mail address: akan@ccmfs.meijo-u.ac.jp (A. Kan).

dielectric properties of MNS were investigated in this study.

2. Experimental method

High-purity ($\geq 99.9\%$) MgO, Nb₂O₅ and Sb₂O₅ powders were prepared using a conventional mixed-oxide route so as to form compounds in Mg₄(Nb_{2-x}Sb_x)O₉ series. After mixing with acetone and calcining at 1100 °C for 20 h in air, these powders were ground with a polyvinyl alcohol and then pressed into a pellet (12 mm in a diameter and 7 mm in thickness) under a pressure of 100 MPa. Subsequently, these pellets were sintered in the temperature range of 1400–1500 °C for 10 h in air. The apparent density of the sample was measured in terms of the Archimedes method. The microwave dielectric properties of the samples were measured by using the Hakki and Coleman method.⁵ The temperature coefficient of resonant frequency of a sample was determined from the resonant frequency at the temperatures of 20 and 80 °C. The crystalline phases of the sintered samples were identified by using the X-ray powder diffraction (XRPD) with the Cu K α radiation; the crystal structure of MNS was refined in terms of the Rietveld analysis;^{6,7} the covalency of the cation-oxygen bond in MNS was evaluated on the basis of the bond valence theorem.^{8,9} Moreover, the electrical structure of MNS was calculated by using the discrete variable X $_{\alpha}$ (DV-X $_{\alpha}$) method,¹⁰ which is one of the first principle calculation methods. Then, the morphological changes in the samples that depended on the composition x were investigated by means of the field emission scanning electron microscopy (FE-SEM) and the energy dispersive X-ray (EDX) analysis.

3. Results and discussion

Fig. 1 shows the XRPD patterns of the MNS ceramics sintered at 1400 °C for 10 h in air. In the composition range of 0–1, a single phase that corresponded to the corundum-type structure was obtained. Moreover, with increasing the composition x from 0 to 1, the diffraction peaks of the samples were shifted to the higher angles of 2θ ; this result was due to the difference in the ionic radii between the Sb⁵⁺ and Nb⁵⁺ ions. In the case of the sintering temperature of 1400 °C, the presence of MgO and Mg₇Sb₂O₁₂ compounds was detected in the XRPD profiles at $x=2$ instead of the formation of the Mg₄Sb₂O₉ compound. Although Kasper et al.¹¹ reported that the single phase of Mg₄Sb₂O₉ compound with ilmenite-type structure was produced at $x=2$, the XRPD patterns of MNS at $x=2$ exhibited the formation of MgO and Mg₇Sb₂O₁₂ compounds as mentioned above because of the different sintering conditions of Mg₄Sb₂O₉ compound with ilmenite-type structure. Thus, from these results, the limit of the solid solutions is considered to be more restrictive than a composition of $x=1$.

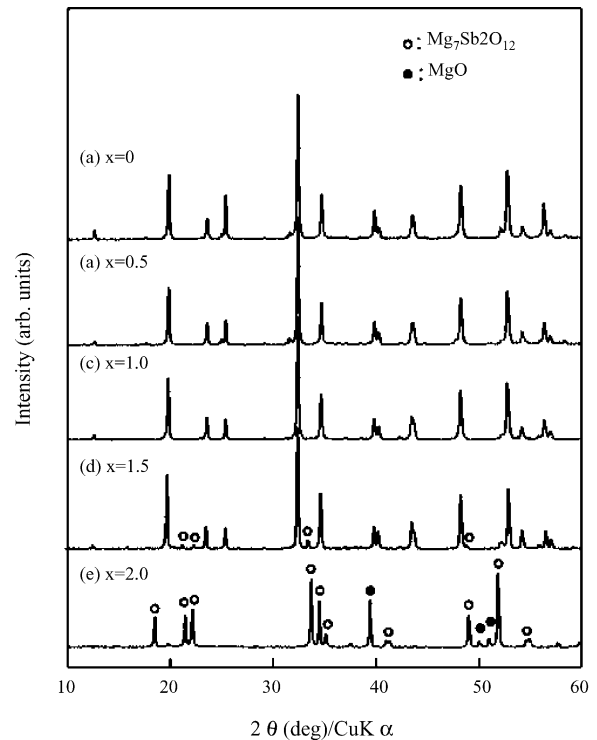


Fig. 1. XRPD patterns of Mg₄(Nb_{2-x}Sb_x)O₉ solid solutions.

In order to clarify the effect of Sb substitution for Nb on the crystal structure of MNS, the lattice parameters of the samples were refined by using the Rietveld method; the relationship between the lattice parameters and the composition x is shown in Fig. 2. In the composition range of 0–1, the lattice parameters of MNS linearly decreased with increasing the composition x because the ionic radius of Sb⁵⁺ ion is small in comparison with that of the Nb⁵⁺ ion.⁴ At the higher compositions than $x=1$, the lattice parameters of MNS were almost constant; therefore, it is considered that the limit of the solid solutions is approximately $x=1$. Although the effect of Sb substitution for Nb on the lattice parameters and the limit of the solid solutions in MNS were clarified by refining the lattice parameters of MNS, the interrelationship among the variations in the atomic distances, the volume of the polyhedra and the lattice parameters of MNS have not been clarified. On the basis of the refined structure parameters in terms of the Rietveld analysis, the bond strength (s) and covalency (f_c) of cation-oxygen bonds were determined by using the following equations:⁸

$$s = \left(\frac{R}{R_0} \right)^{-N} \quad (1)$$

$$f_c = as^M \quad (2)$$

where R and R_0 represent the atomic distance obtained in this study and the empirical parameter, respectively; N is constant ($N=4.29$ for Mg, and $N=6.0$ for Nb and Sb). In this case, the R_0 values of Mg, Nb and Sb were 1.622, 1.907 and 1.911, respectively.⁹ Moreover, in the Eq. (2), the parameters, a and

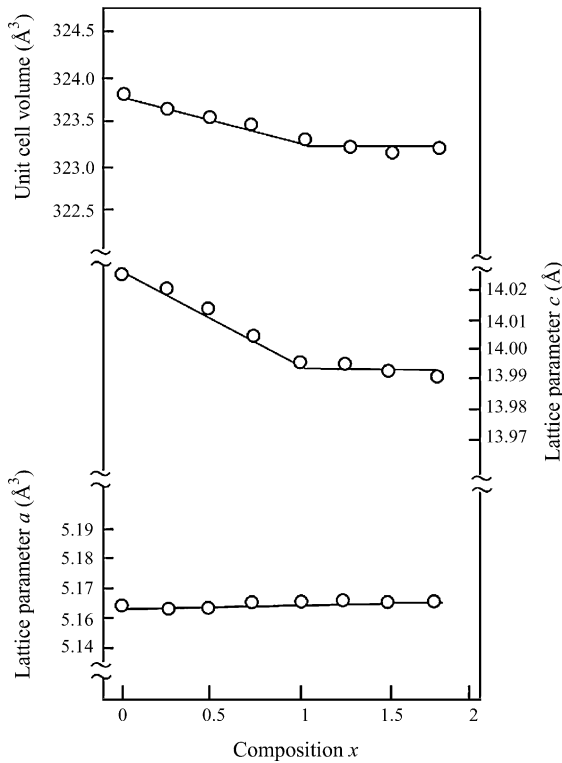


Fig. 2. Lattice parameters of $Mg_4(Nb_{2-x}Sb_x)O_9$ solid solutions as a function of composition x .

M , depend on the number of electrons in each cation; the values of a and M for Mg and Sb are 0.49 and 1.57, whereas those of Nb are 0.67 and 1.43, respectively.⁸ The influence of Sb substitution for Nb on the normalized covalency of cation-oxygen bonds in the composition range of 0–1 is shown in Fig. 3. Since any remarkable differences in the normalized covalency of Mg–O bond were not observed, the covalency of Mg–O bond in the MgO_6 octahedra is independent of the Sb substitution for Nb. On the other hand, in the cases of the Sb–O and Nb–O bonds, the normalized covalency of Sb–O bond at $x = 1$ was higher than that of the Nb–O bond at $x = 0$. Thus, it was found that the Sb substitution for Nb enhanced the covalency of Sb–O bond in the SbO_6 octahedron, though the covalency of Mg–O bonds in the MgO_6 octahedra was approximately constant in both the samples at $x = 0$ and 1.

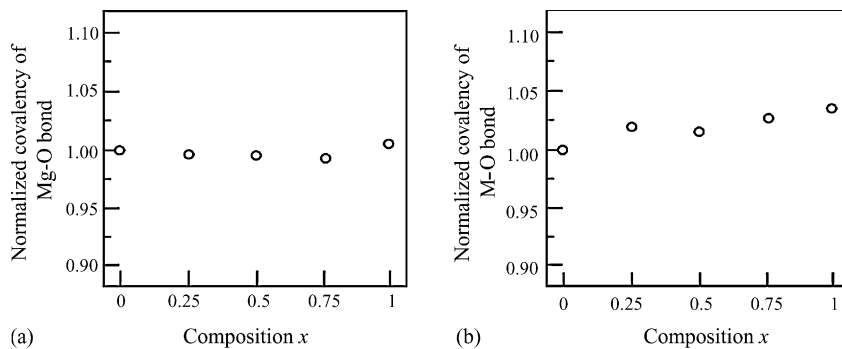


Fig. 3. Normalized covalency of Mg–O and M–O ($M = Nb$ and Sb) bond as a function of composition x .

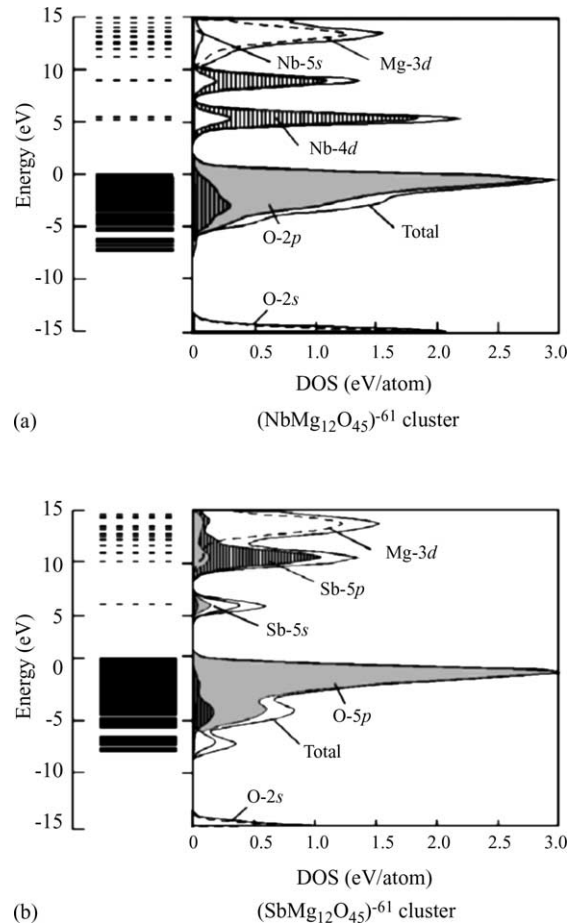


Fig. 4. Energy level diagrams and total and partial density of states of (a) $Mg_4Nb_2O_9$, (b) $Mg_4Sb_2O_9$ by $(AMg_{12}O_{45})^{-61}$ ($A = Nb$ and Sb) cluster.

Total density of states (DOS) and partial DOS of the Nb- and Sb-centered cluster models are shown in Fig. 4a and b with the energy level diagrams. In both of the energy level diagrams, the filled bands located from -7 to 0 eV are mainly composed of the O-2p orbitals. The unoccupied bands of $(NbMg_{12}O_{45})^{-61}$ cluster model located above 5 eV are made up of Nb-4d, Nb-5s and Mg-3d orbitals, whereas those of $(SbMg_{12}O_{45})^{-61}$ cluster model located higher than 6 eV are constituted of Sb-5s, Sb-5p and Mg-3d orbitals. Since the Mg-3d orbitals in DOS of both cluster models have very small

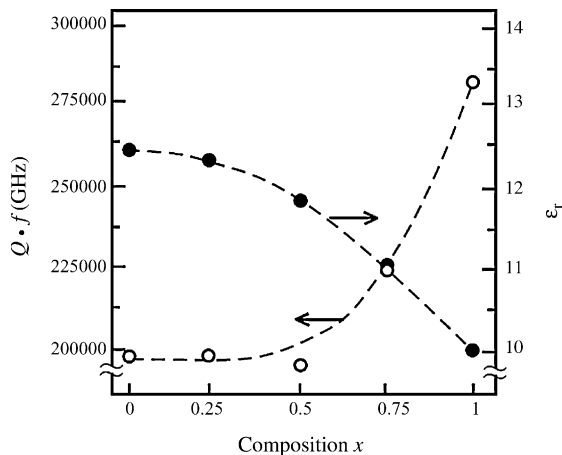


Fig. 5. Dielectric constants (ϵ_r) and $Q \cdot f$ values of $\text{Mg}_4(\text{Nb}_{2-x}\text{Sb}_x)\text{O}_9$ solid solutions as a function of composition x .

contributions to the valence band, Mg in the cluster models is considered to be nearly completely ionized. The alternative Nb-4*d* and Sb-5*p* states in the O-2*p* band are found a little in both modes; the mixture of Nb-4*d* and Sb-5*s* states in the O-2*p* band suggests the strong covalent interaction between pentavalent cations (Nb and Sb) and oxygen. These results indicate that Mg atoms are substantially in the Mg^{2+} state and have the slight covalency with the surrounding atoms. Thus, the location of Mg^{2+} does not exert an influence on the electronic states of the clusters. The net charges, which define the ionicity of the atoms, for the Nb and Mg ions at $x=0$ were 2.55 and 1.81, respectively, and those of the Sb and Mg ions at $x=2$ were 2.55 and 1.82, respectively. Thus, the covalent interactions of the Nb–O and Sb–O bonds are considered to be strong and the Mg–O bond at $x=0$ and 2 may be an ionic interaction. From these results, it is considered that the Sb substitution for Nb in MNS exerts an influence on the average bond strength of the Nb–O and Sb–O bonds in the NbO_6 and SbO_6 octahedra. The bond order, which represents the strength of covalent Nb–O and Sb–O bonds in the NbO_6 and SbO_6 octahedra, was determined in order to discuss the covalent interactions in more detail. The bond order of Sb–O bond (0.180) is larger than that of the Nb–O bond (0.133), whereas those of the Mg–O bond in MgIO_6 and Mg_2O_6 octahedra were unchanged by Sb substitution for Nb. From these results, it was clarified that the Sb–O bond became more covalent than the Nb–O bond.

Fig. 5 shows the variations in the dielectric constant of MNS sintered at 1400 °C for 10 h in air as a function of composition x . The dielectric constant of MNS with the composition x ranging from 0 to 1 slightly decreased from 13 to 10. Since the relative densities of MNS in the single phase region ($0 \leq x \leq 1$) were approximately 93% of the theoretical density, it is considered that the sintering temperature dependence on the sintability of MNS in the composition range of 0–1 is small. At the range of microwave frequencies, the dielectric constant of ceramics is known to be effected by the ionic polarizability of the cations; Shannon reported the

various ionic polarizabilities of the cations.¹² It is suggested that an increase in the dielectric constant takes place with the Sb substitution for Nb because the ionic polarizability of Sb^{5+} ion (4.27 \AA^3) is larger than that of Nb^{5+} ion (3.97 \AA^3).¹² The dielectric constant of MNS in the composition range of 0–1, however, decreased as shown in Fig. 5. Therefore, the variation in the dielectric constant of MNS is considered to extremely depend on the crystal structure of MNS; in a previous work,² it suggests that the enhanced covalency of Ta–O bond in the octahedron by the Ta substitution for Nb lowers the dielectric constant of MNT. From the calculation of the covalency in MNS, it was found that the covalency of Sb–O at $x=1$ was higher than that of Nb–O bond at $x=0$ as mentioned above. Moreover, Guo et al.¹³ also suggested that the difference in the dielectric constant between the $\text{Sr}(\text{Al}_{1/2}\text{Nb}_{1/2})\text{O}_3$ and $\text{Sr}(\text{Al}_{1/2}\text{Ta}_{1/2})\text{O}_3$ ceramics is due to the variations in the bond strength of Nb–O and Ta–O bonds. Thus, the decrease in the dielectric constant of MNT in the single phase region may relate to the variations in the covalency of Sb–O and Nb–O bonds in the AO_6 octahedra.

The variations in the $Q \cdot f$ values of MNS are also shown in Fig. 5 as a function of composition x . The $Q \cdot f$ values of MNS increased from 193,000 to 283,000 GHz in the single phase region; the maximum $Q \cdot f$ value was obtained at $x=1$. The improvement in $Q \cdot f$ value of MNS in the single phase region exhibited a similar tendency to those of MNT.² In a previous work,² the covalency-microwave dielectric property relations in MNT were discussed; it suggests that the Ta substitution for Nb in MNT takes place the increases in the covalency of the Ta–O bond and $Q \cdot f$ value. In this study, the Sb substitution for Nb also enhanced the covalency of Sb–O bond, and the $Q \cdot f$ values of MNS increased, depending on the composition as mentioned above. Thus, it is considered that the variations in covalency of the Sb–O and Nb–O bonds may exert an influence on the $Q \cdot f$ value of MNS. Moreover,

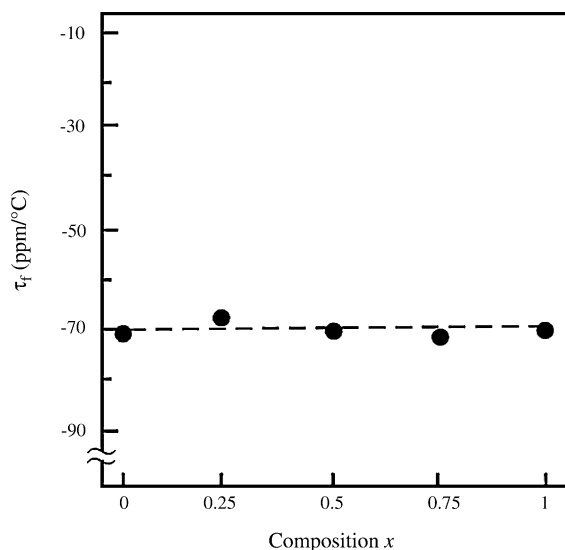


Fig. 6. Temperature coefficient of resonant frequency (τ_f) of $\text{Mg}_4(\text{Nb}_{2-x}\text{Sb}_x)\text{O}_9$ solid solutions as a function of composition x .

the $Q:f$ values of MNS at the compositions higher than $x = 1$ decreased from 280,000 to 50,000 GHz because of the formation of secondary phases as mentioned above. Thus, the Sb substitution for Nb is effective in improving the $Q:f$ values in this system as well as the Ta substitution for Nb in MNT.²

The influence of the Sb substitution for Nb in MNS on the temperature coefficient of resonant frequency is shown in Fig. 6; the τ_f values of MNS ranged from -70 to 8 ppm/ $^{\circ}$ C. In the single phase region ($0 \leq x \leq 1$), a significant variation in the τ_f values was not recognized; these values were approximately constant. Therefore, it is considered that the Sb substitution for Nb basically does not exert an influence on the τ_f value of MNS in the single phase region.

4. Conclusions

The microwave dielectric properties of $\text{Mg}_4(\text{Nb}_{2-x}\text{Sb}_x)\text{O}_9$ solid solutions were evaluated and the variations in the electric state of the solid solutions were investigated by using the first principle calculation method. The formation of a single phase was observed from the X-ray powder diffraction patterns of the solid solutions sintered at 1400°C in the composition range of $0-1$. The MgO and $\text{Mg}_7\text{Sb}_2\text{O}_{12}$ were detected as the secondary phases at the compositions higher than $x = 1$. Comparing the overlap population of the $(\text{NbMg}_{12}\text{O}_{45})^{-61}$ cluster model with that of the $(\text{SbMg}_{12}\text{O}_{45})^{-61}$ cluster model, the slight covalency of the Sb–O bond was recognized from the results of the first principle calculation method. In the composition range of $0-1$, the $Q:f$ values of $\text{Mg}_4(\text{Nb}_{2-x}\text{Sb}_x)\text{O}_9$ solid solutions sintered at 1400°C increased from 196,000 to 280,000 GHz; the dielectric constants of the solid solutions ranged from 13 to 10. However, an improvement in the temperature coefficient of resonant frequency by the Sb substitution for Nb was not recognized.

References

1. Breeze, J., Penn, S. J., Poole, M. and Alford, N. McN., Layered $\text{Al}_2\text{O}_3\text{-TiO}_2$ composite dielectric resonators. *Electron. Lett.*, 2000, **36**, 883–884.
2. Ogawa, H., Kan, A., Ishihara, S. and Higashida, Y., Crystal structure of corundum type $\text{Mg}_4(\text{Nb}_{2-x}\text{Ta}_x)\text{O}_9$ dielectric ceramics with low dielectric loss. *J. Eur. Ceram. Soc.*, 2003, **23**, 2485–2488.
3. Kan, A., Ogawa, H., Yokoi, A. and Ohsato, H., Low-temperature sintering and microstructure of $\text{Mg}_4(\text{Nb}_{2-x}\text{V}_x)\text{O}_9$ microwave dielectric ceramic by V substitution for Nb. *Jpn. J. Appl. Phys.*, 2003, **42**, 6154–6157.
4. Shannon, R. D., Revised effective ionic radii and systematic studies of interatomic distances in halides and chalcogenides. *Acta Cryst.*, 1976, **A32**, 751–767.
5. Hakki, B. W. and Coleman, P. D., A dielectric resonator method of measuring inductive capacities in the millimeter range. *IRE Trans. Microwave Theory Tech.*, 1960, **MTT-8**, 402–410.
6. Rietveld, H. M., A profile refinement method for nuclear and magnetic structures. *J. Appl. Crystallogr.*, 1969, **2**, 65–71.
7. Izumi, F., *Rietveld Method*, ed. R. A. Young. Oxford University Press, Oxford, 1993, Chapter 13.
8. Brown, I. D. and Shannon, R. D., Empirical bond-strength–bond-length curves for oxides. *Acta Cryst.*, 1973, **A29**, 266–282.
9. Brown, I. D. and Wu, K. K., Empirical parameters for calculating cation–oxygen bond valences. *Acta Cryst.*, 1976, **B32**, 1957–1959.
10. Adachi, H., Tsukada, M. and Satoko, C., Discrete variational $X\alpha$ cluster calculations. I. Application to metal clusters. *J. Phys. Soc. Jpn.*, 1978, **45**, 875–883.
11. Kasper, H., Ilmenite type phases in the magnesium oxide–antimony pentoxide (Sb_2O_5) system and light absorption of divalent nickel and cobalt cations in the magnesium antimony oxide [$\text{Mg}_7\text{Sb}_2\text{O}_{12}$]. *Z. Kristallogr.*, 1968, **128**, 72–84.
12. Shannon, R. D., Dielectric polarizabilities of ions in oxides and fluorides. *J. Appl. Phys.*, 1993, **73**, 348–366.
13. Guo, R., Bhalla, A. S., Sheen, J., Ainger, F. W., Erdei, S., Subbarao, E. S. et al., Strontium aluminum tantalum oxide and strontium aluminum niobium oxide as potential substrate for HTSC thin films. *J. Mater. Res.*, 1995, **10**, 18–25.